ELECTRON BEAM CHARGING OF SPACE SHUTTLE THERMAL PROTECTION SYSTEM TILES

John V. Staskus
National Aeronautics and Space Administration
Lewis Research Center
Cleveland, Ohio 44135

Six space shuttle reusable surface insulation tiles were tested in the NASA Lewis Research Center's electron bombardment test facility. The 30-cm-square specimens were assembled by using the same materials and techniques used to apply the tiles to the space shuttle and were composed of 15-cm- and 20-cm-square tiles and pieces on 0.6-cm-thick aluminum substrates. There were two specimens of each of three thicknesses. One specimen of each thickness had gaps of less than 0.1 cm between tiles, and the other had gaps of approximately 0.15 cm. The specimens were exposed to monoenergetic electron beams (2 to 25 keV) with nominal fluxes of 0.1 and 1 nA/cm^2. Tests were conducted with both grounded and floating substrates. The data presented include charging rates, equilibrium potentials, and substrate currents. There is evidence that discharging occurred.

INTRODUCTION

The advent of polar orbit space shuttle missions has raised new concerns about spacecraft charging - concerns formerly associated with high-altitude (i.e., geosynchronous) satellites. Charging of dielectric materials by multi-kilovolt-energy electrons can cause arc discharging, which may result in rf noise that can interfere with communications and may induce voltage transients in the electrical system that can upset or damage low-level electronic circuitry. At the request of the Air Force Geophysics Laboratory and with specimens supplied by the NASA Johnson Space Center low-keV electron beam charging tests were conducted in the electron bombardment test facility at the NASA Lewis Research Center.

Tests conducted previously at the Rome Air Development Center investigated the response of shuttle tile materials to electron beams with energies from 10 keV to 1 MeV (ref. 1). In that work discharges were detected as current pulses to a substrate. This work investigated the charging behavior of surface insulation tiles from the shuttle's thermal protection system (described in refs. 2 to 4) when subjected to monoenergetic electron beams with energies of 2 to 25 keV.

TEST SPECIMENS

The test specimens provided by Johnson consisted of 0.6-cm-thick by 30-cm-square aluminum plates with shuttle tile pieces attached. The materials and techniques used were the same as those used to apply the tiles to the space shuttle. There were two specimens of each of three thicknesses (1-1/4 cm,

2-1/2 cm, and 5 cm). The thinnest tiles (20 cm square) were white and the others (15 cm square) were black. One specimen of each thickness had gaps of less than 0.1 cm between tile pieces and the other had gaps of approximately 0.15 cm. Each specimen contained at least one full uncut tile. Most of the tile pieces had 3x5 dot matrix identification code characters stenciled on them - black on the white tiles and yellow on the black tiles. The 5-cm-thick specimen with large gaps had a filler material that appeared to be folded glass fabric in the gaps, with the fold at the exposed surface. Figures 1 to 9 show edges and faces of the six specimens. Capacitances measured from a conductive sheet placed on the tiles to the aluminum substrate were approximately 75 pF for the 1-1/4-cm-thick tile specimens, 50 pF for the 2-1/2-cm-thick specimens, and 30 pF for the 5-cm-thick specimens.

CONFIGURATION AND TESTS

The specimens were tested individually in the 2-m-long by 2-m-diameter electron bombardment test facility (ref. 5). They were mounted approximately 1.2 m from the electron source with the specimen's face normal to the source-target axis. The substrate was supported on Lucite posts so that tests could be conducted with the substrate floating as well as grounded. In the grounded substrate configuration an electrometer was used to monitor substrate current collection. The edges and rear of the substrate, which were not covered with shuttle tiles, were covered with Kapton to minimize the substrate's collection of particles other than the beam electrons intercepted by the irradiated surface.

The capacitance measured between the substrate and its vacuum chamber environment was approximately 20 pF. This would also be an upper limit to the capacitance expected between the exposed tile face and the chamber environment in parallel with the 30- to 75-pF capacitance across the tile to the substrate.

Noncontacting electrostatic voltage probes were used to measure potentials across the tile surface and on the substrate when it was floating. For early tests a single probe was available and was swept across the tile surface at a separation of approximately 0.2 cm. When the substrate was floating, a small patch of metal connected to the substrate was placed in the path of the probe in order to monitor the substrate's potential. The patch was shielded from direct interception of beam electrons, but the substrate was less well isolated from other particles in its environment. For later tests a second probe continuously monitored the substrate from behind.

The tests consisted of exposing the specimens to monoenergetic electron beams of 2-,5-,10-,15-,20-, and 25-keV energy with nominal fluxes of 0.1 and 1 nA/cm^2. The data presented herein consist of current to the specimen substrate read with an electrometer, potential profiles across the sample obtained by periodically sweeping a noncontacting voltage probe across the specimen's face, and time-exposure photographs of the irradiated surface made with a camera located outside one of the vacuum chamber windows.

RESULTS

A typical test began with exposure of the specimen to the electron beam while the voltage probe was sweeping across the tile surface. This gave an

indication of the charging rate of the uncharged surface during the initial seconds of exposure. A single point on the surface could not be monitored continuously as the presence of the voltage probe would shield that point from charging by the electron beam. Generally the tile surface was charged to nearly its equilibrium potential in less than 1 min from the time of initial exposure. Figure 10 illustrates the charging behavior. It shows the charging of one of the thinnest, highest capacitance specimens for two electron beams with order-of-magnitude different fluxes. As would be expected, there is approximately an order-of-magnitude difference in the time taken to reach a given potential in the two beams. Figure 11 presents the equilibrium surface potentials as a function of beam energy for the six specimens. The range of potentials observed across a specimen's surface is indicated by symbols joined with a vertical line. The charging of the tile surfaces to within 2 kV of the beam accelerating potential suggests that the secondary electron emission coefficient's second crossing of unity occurs at approximately 2 kV (ref. 6). Table I presents the substrate currents for the six specimens at the ends of the tests.

An interesting observation made in some of the tests was that the potential of the dot matrix characters on the tile was sometimes greater than the beam accelerating potential. This could conceivably occur if the secondary electron coefficient of the character paint were sufficiently less than that of the surrounding tile. The characters would rapidly charge negative relative to the surrounding tile. Then if the charging rate of the surrounding tile were rapid enough, the potential difference between the characters and tile could be maintained, carrying the characters to potentials greater than the beam accelerating potential. This kind of behavior has been observed in the charging of dielectrics on metallic substrates that were initially grounded and then permitted to float (ref. 7).

Figure 12, a 15-min time-exposure photograph for a 25-keV, 1-nA/cm^2 irradiation, shows the optical evidence of discharging that takes place on the tile surfaces with the substrate grounded. The activity was not visible to the eye and was not apparent in the substrate current being monitored. The fuzzy illumination along the gaps between tiles was barely evident in the photograph made at 15 keV and 1 nA/cm^2 but became brighter with increasing beam energy. Fifteen-minute time exposures made with the electron flux at 0.1 nA/cm^2 do not show the discharging along the gaps. Photographs with an order-of-magnitude longer exposure were not attempted since the discharging activity was not the only source of light in the chamber: the electron gun, though designed to minimize it, produced a low level of illumination. The activity along the tile gaps could be reduced by inserting a dielectric barrier in the gap, as was done with the 1-1/4-cm-thick specimen having the wide gaps between tiles. Figure 13 shows the locations of the barrier materials as well as time-exposure photographs made before and after addition of the barriers.

Results from tests with the substrate floating seem to indicate that the discharging was dependent on the potential difference across the tile from its exposed face to its substrate. In all of those tests, the one specimen that did not exhibit the optical evidence of discharging was the one for which that potential difference never exceeded 3 kV. The other five specimens produced evidence of discharging in the 15- to 25-keV beam energy range, where the surface-to-substrate potential difference usually exceeded 10 kV. Some photographs showed discharging taking place along the outer edges of the specimens as well as along the gaps between tiles. None of the photographs indicated

anything taking place away from the edges near the center of any uncracked tile or segment of tile. Figure 14 shows the potentials as a function of beam energy for the six specimens tested with their substrates floating.

An experiment was conducted in which an edge of one of the thickest specimens was irradiated. One-half of the edge had the hard borosilicate glass skin of the finished edge of a tile and the other half had the exposed low-density silica fiber bulk tile material of a tile that had been cut. The specimen was positioned so that the voltage probe swept across both materials as far as 3 cm away from the grounded substrate. Figure 15 presents the surface potentials observed as a function of beam energy. The borosilicate material charged to potentials observed in the earlier testing. The silica fiber material charged to no more than 13 percent of the beam accelerating potential for any test and is probably the result of high secondary electron emission (ref. 1). Figure 16, a time-exposure photograph, shows glowing silica fiber material and discharging in or across the nylon fiber strain isolation pad (SIP) located between the tiles and the grounded aluminum substrate.

When the substrate was permitted to float, the borosilicate surface charged to the same potentials as before. The silica fiber material became somewhat more negative than when the substrate was grounded but was now positive with respect to the substrate - the substrate being nearly as negative as the borosilicate surface. Figure 17 shows the potentials as a function of beam energy, and figure 18 is a time-exposure photograph showing little discharging in or across the SIP. Time-exposure photographs made immediately following the 25-keV exposure gave no indication of continuing activity after the electron beam was turned off. However, in the tests with the substrate grounded the electrometer sensitivity was increased after the electron beam was turned off, and a non-exponential-decaying positive current was detected as well as positive current spikes whose frequency of occurrence decreased with time. The current read immediately after electron beam turnoff was approximately 0.4 nA, decaying to 0.04 nA at 160 s and to 0.004 nA at 925 s.

CONCLUDING REMARKS

When subjected to monoenergetic electron beams, the space shuttle thermal protection system tiles rapidly charged to potentials about 2 kV less in magnitude than the beam accelerating voltage. This is indicative of a secondary electron emission coefficient second-crossover potential of approximately 2 kV. Optical evidence of surface discharge activity was produced for beam energies of 15 keV and greater and is concentrated along gaps between tiles and cracks in the glass skin. The intensity of the activity appeared to be dependent on the potential difference between the exposed tile surface and the tile's substrate. Evidence of discharging was not seen when that potential difference was 3 kV or less. Placing a barrier of high-voltage-insulating material such as Kapton or Teflon in the gaps between tiles reduced the discharging along the gaps. The potentials achieved on the bulk tile material during the edge irradiation were quite low and suggest that the silica fiber material has a high secondary electron emission yield in contrast to the highly insulating glass skin. In addition, discharge activity was detected to occur at a decaying rate after the electron irradiation source was turned off.

REFERENCES

1. Frederickson, A. R.; and Chesley, A. L.: Charging/Discharging of Space Shuttle Tile Material Under Irradiation. IEEE Trans. Nucl. Sci., vol. 30, no. 6, Dec. 1983, pp. 4296-4301.

2. Dotts, Robert L.; Smith, James A.; and Tillian, Donald J.: Space Shuttle Orbiter Reusable Surface Insulation Flight Results. Shuttle Performance: Lessons Learned, J. P. Arrington and J. J. Jones, eds., NASA CP-2283, Part 2, 1983, pp. 949-966.

3. Banas, Ronald P., et al.: Lessons Learned from the Development and Manufacture of Ceramic Reusable Surface Insulation Materials for the Space Shuttle Orbiters. Shuttle Performance: Lessons Learned, J. P. Arrington and J. J. Jones, eds., NASA CP-2283, Part 2, 1983, pp. 967-1008.

4. Cooper, Paul A.; and Sawyer, James Wayne: Life Considerations of the Shuttle Orbiter Densified-Tile Thermal Protection System. Shuttle Performance: Lessons Learned, J. P. Arrington and J. J. Jones, eds., NASA CP-2283, Part 2, 1983, pp. 1009-1024.

5. Berkopec, F. D.; Stevens, N. J.; and Sturman, J. C.: The Lewis Research Center Geomagnetic Substorm Simulation Facility. Proceedings of the Spacecraft Charging Technology Conference, C. P. Pike and R. R. Lovell, eds., NASA TM-73537 and AFGL TR-77-0051, 1977, pp. 423-430.

6. Jenkins, Ronald Osmond; and Trodden, W. G.: Electron and Ion Emission from Solids. Dover Publications, Inc., 1965.

7. Purvis, C. K., et al.: Charging Rates of Metal-Dielectric Structures. Spacecraft Charging Technology - 1978, Robert C. Finke and Charles P. Pike, eds., NASA CP-2071 and AFGL TR-79-0082, 1979, pp. 507-523.

TABLE I. - EQUILIBRIUM SUBSTRATE CURRENTS

Beam energy, keV	1-1/4-cm-thick tiles				2-1/2-cm-thick tiles				5-cm-thick tiles			
	Minimum gap		Wider gap		Minimum gap		Wider gap		Minimum gap		Wider gap	
	Flux, nA/cm^2	Equilibrium substrate current, nA	Flux, nA/cm^2	Equilibrium substrate current, nA	Flux, nA/cm^2	Equilibrium substrate current, nA	Flux, nA/cm^2	Equilibrium substrate current, nA	Flux, nA/cm^2	Equilibrium substrate current, nA	Flux, nA/cm^2	Equilibrium substrate current, nA
2	-0.145 -1.19	-0.026 -.226	-0.132 -1.25	-0.09 -.1	-0.107 -.81	0.07 .03	-0.102 -1.16	-0.016 -.125	-0.075 -1.01	0.028 .064	-0.1 -.64	0.076 .083
5	-0.17 -2.59	-3.5 -17	-0.082 -1	-2.6 -1.8	-0.088 -1	-0.7 -2	-0.144 -.6	-6 -41.7	-0.09 -1.03	-0.5 -4.5	-0.1 -1.04	-0.57 -.22
10	-0.166 -1.86	-9 -82.4	-0.092 -.72	-7 -73	-0.09 -.82	-6 -55.8	-0.101 -1.16	-7 -79	-0.094 -.92	-7.4 -109	-0.088 -1.29	-2 -8
15	-0.126 -1.054	-9 -73.7	-0.104 -.855	-7.5 -111.3	-0.09 -.95	-6 -75.8	-0.106 -1.05	-8 <-79	-0.085 -.95	-10 -107	-0.105 -.66	-2.2 -10
20	-0.145 -1.19	-4.6 -74.3	-0.103 -.94	-9 -98	-0.095 -1.09	-4.9 -70	-0.117 -1.138	-8.8 <-85.5	-0.085 -.94	-9.3 -99	-0.1 -.96	-7.2 -50
25	-.35 -1.305	-10.6 -87.8	-0.136 -.94	-10 -76.7	-0.09 -.995	-5 -51.5	-0.127 -1.12	-8.1 <-71.3	-0.093 -1.05	-7 -94	-0.1 -.814	-8 -68

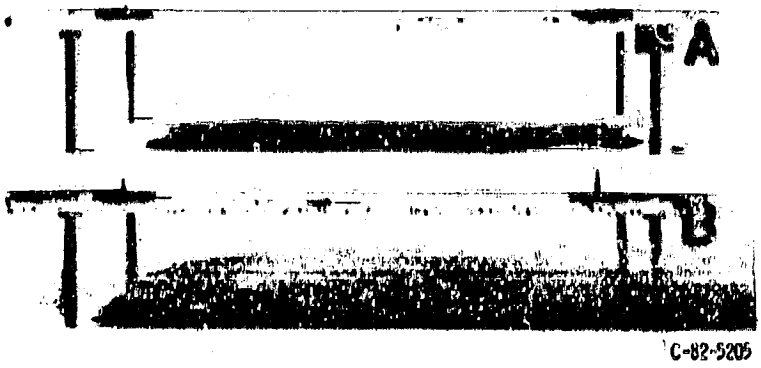

Figure 1. - Edge view of 1-1/4-cm-thick tile specimens A and B.

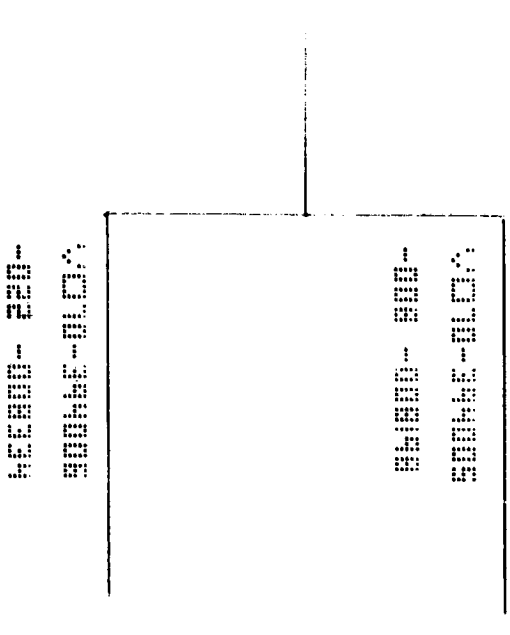

Figure 2. - Face of 1-1/4-cm-thick tile specimen A.

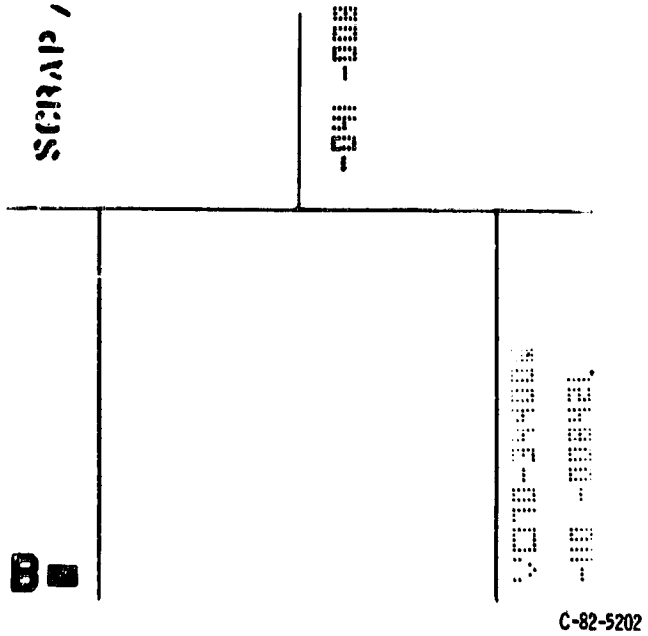

Figure 3. - Face of 1-1/4-cm-thick tile specimen B.

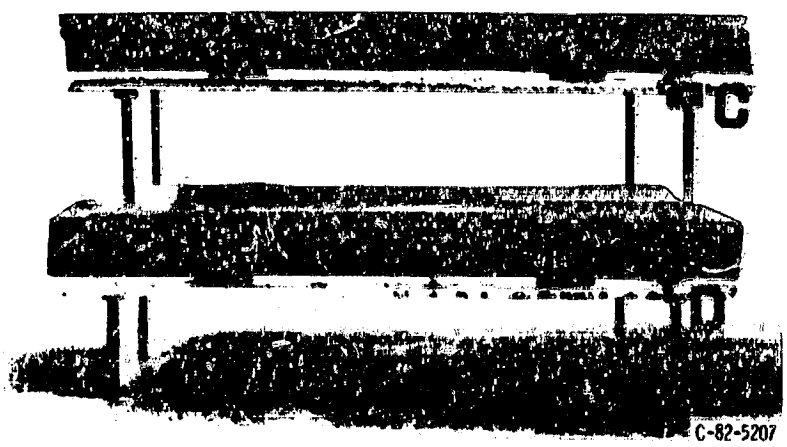

Figure 4. - Edge view of 2-1/2-cm-thick tile specimens C and D.

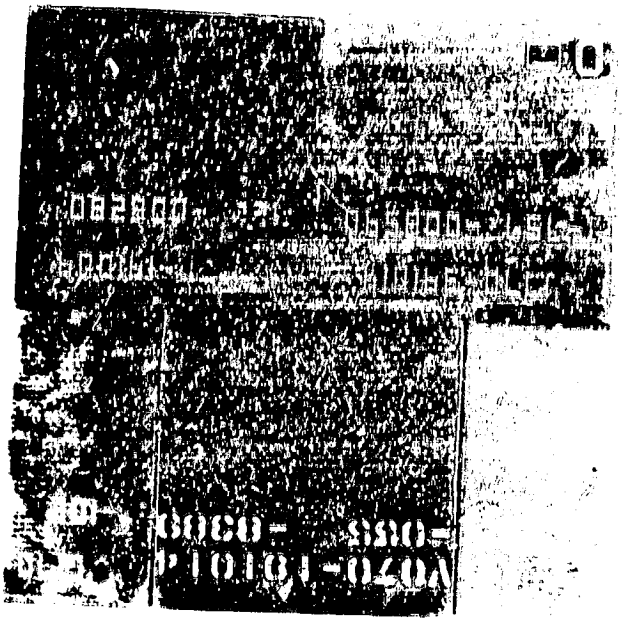

C-82-5201

Figure 5. - Face of 2-1/2-cm-thick tile specimen C.

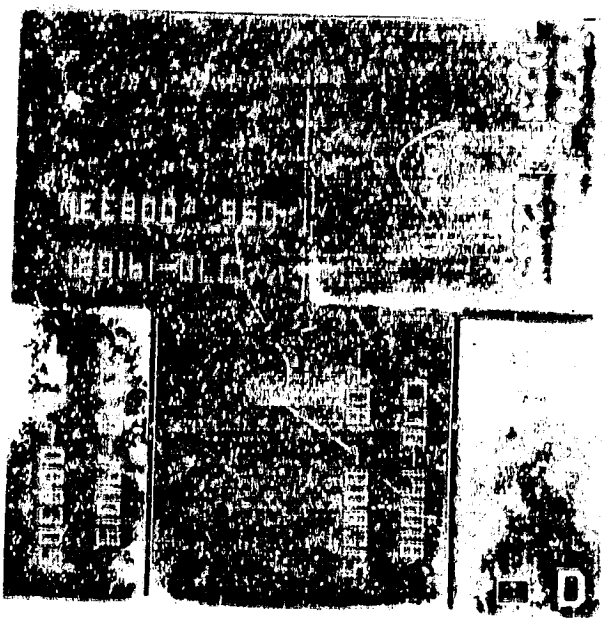

C-82-5203

Figure 6. - Face of 2-1/2-cm-thick tile specimen D.

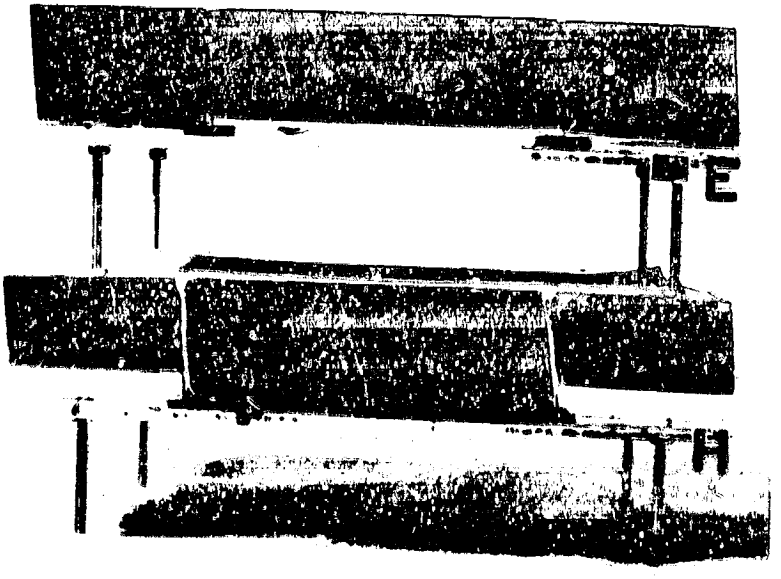

C-82-5206

Figure 7. - Edge view of 5-cm-thick tile specimens E and H.

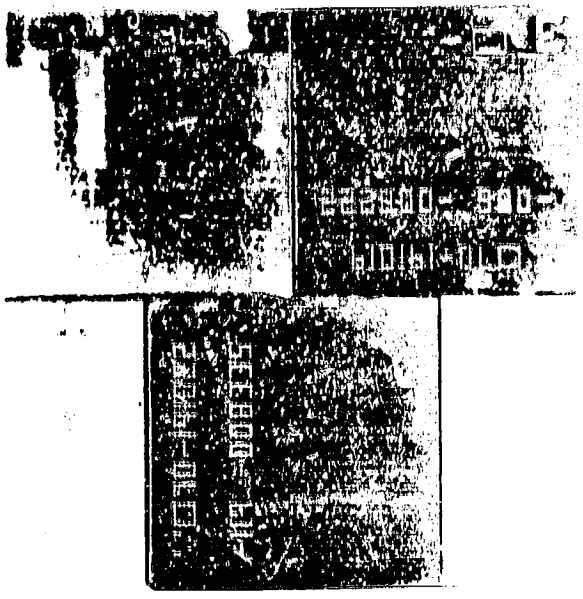

C-82-5200

Figure 8. - Face of 5-cm-thick tile specimen E.

C-82-5199

Figure 9. - Face of 5-cm-thick tile specimen H.

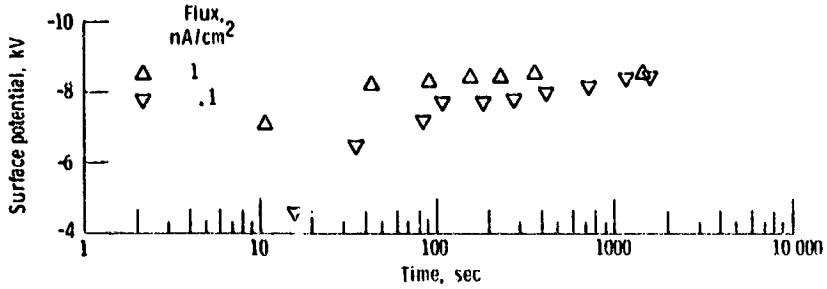

Figure 10. - Electron beam charging of 1-1/4-cm-thick shuttle tile specimens - 10-keV beams.

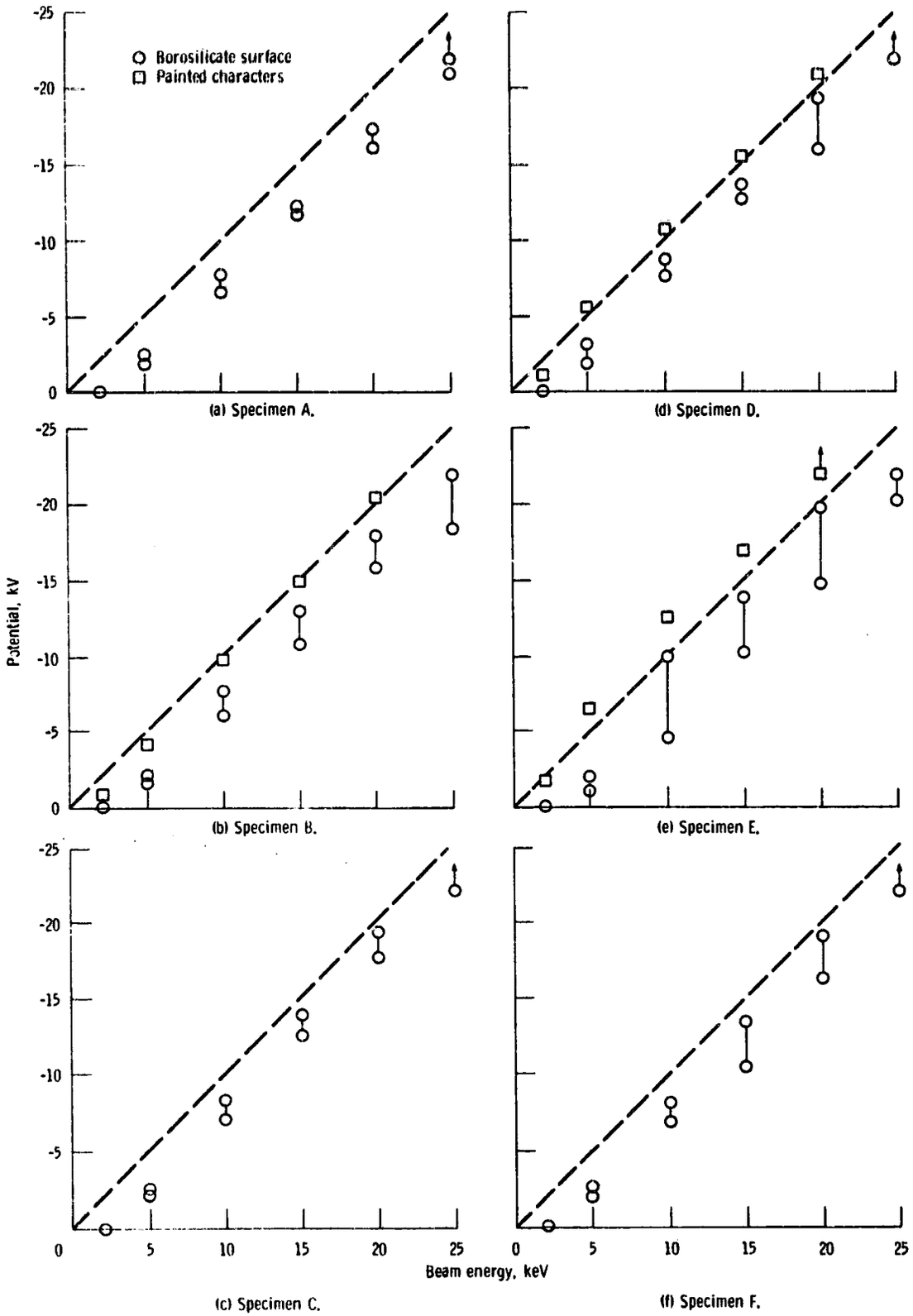

Figure 11. - Potential as a function of beam energy. Flux, 1 nA/cm^2.

Figure 12. - Time exposure of discharging along shuttle tile gaps.

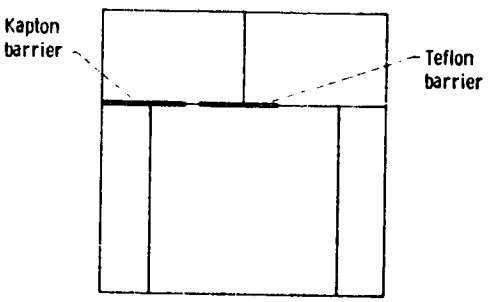

(a) Location of Kapton and Teflon gap barrier strips.

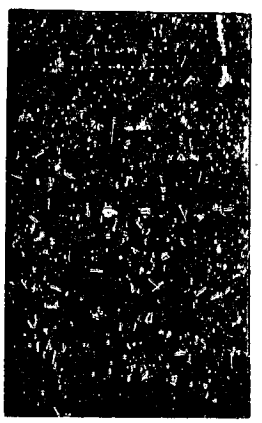

(b) Discharging before installation of dielectric gap fillers.

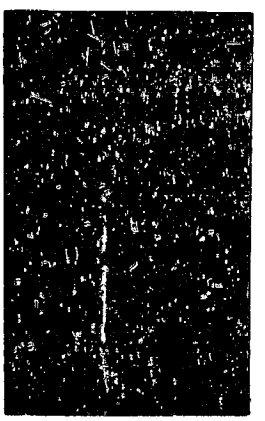

(c) Discharging after installation of dielectric gap fillers.

Figure 13. - Barrier strips.

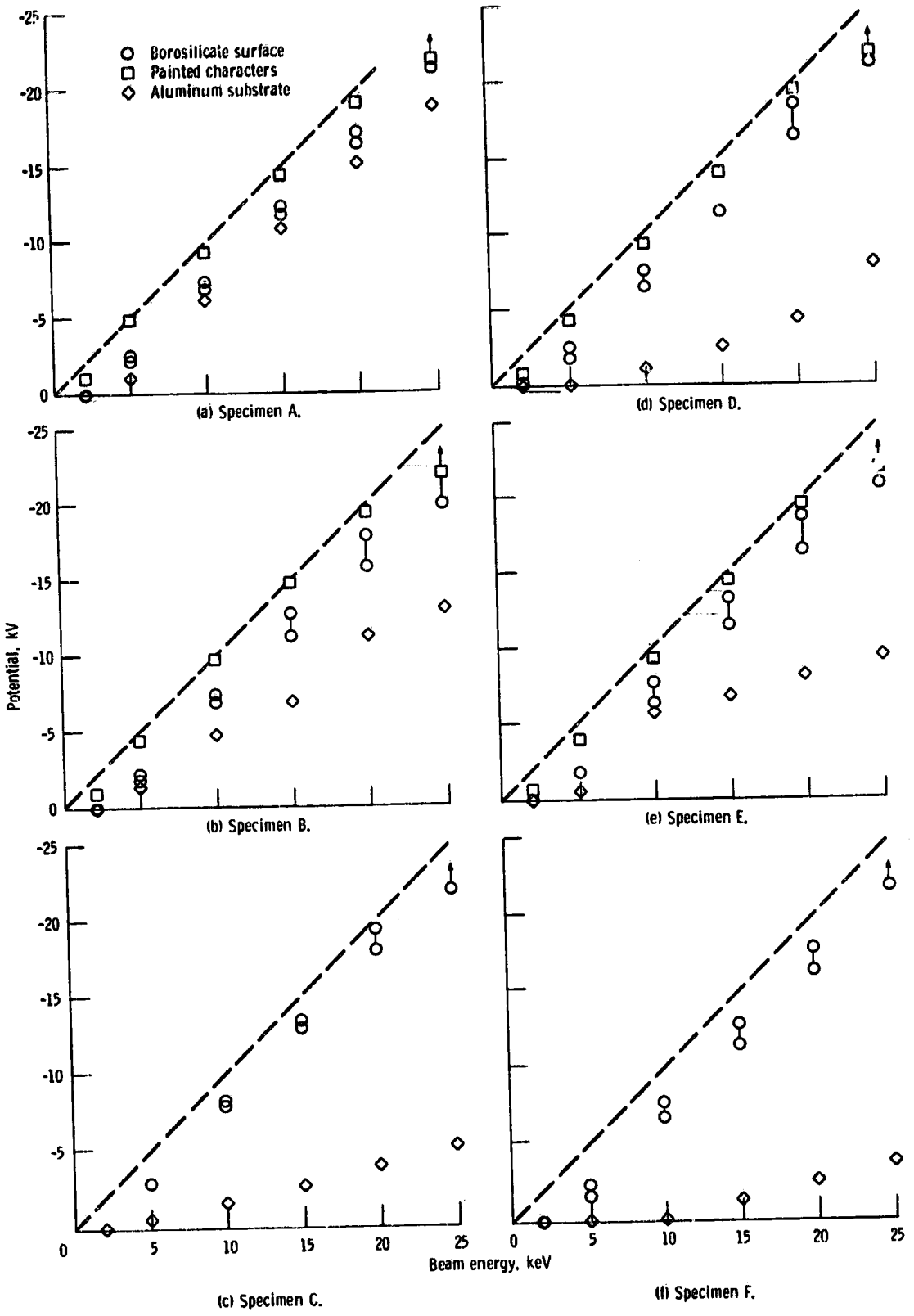

Figure 14. - Potential as a function of beam energy - floating substrate.

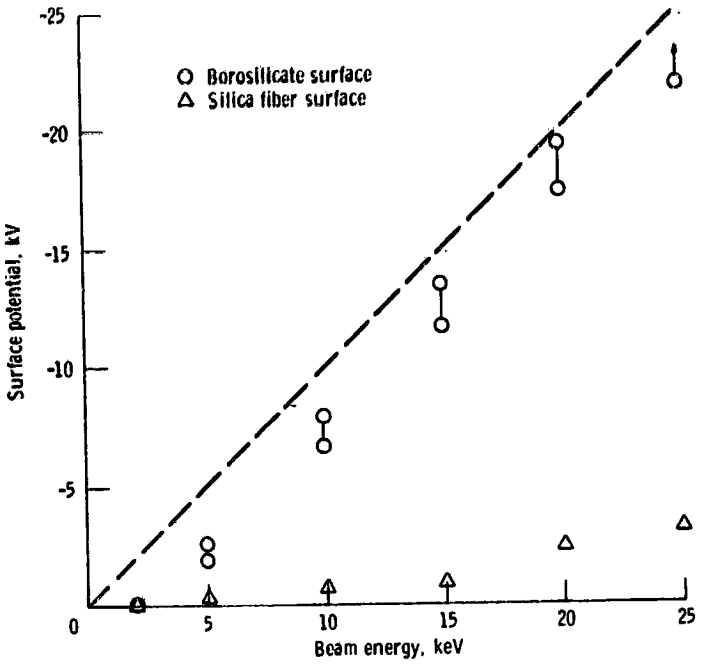

Figure 15. - Surface potential as a function of beam energy - substrate grounded.

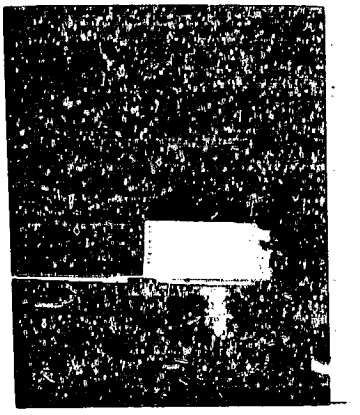

Figure 16. - 15-Minute time exposure of edge-irradiated specimen - substrate grounded. Beam energy, 25 keV; flux, 1 nA/cm^2.

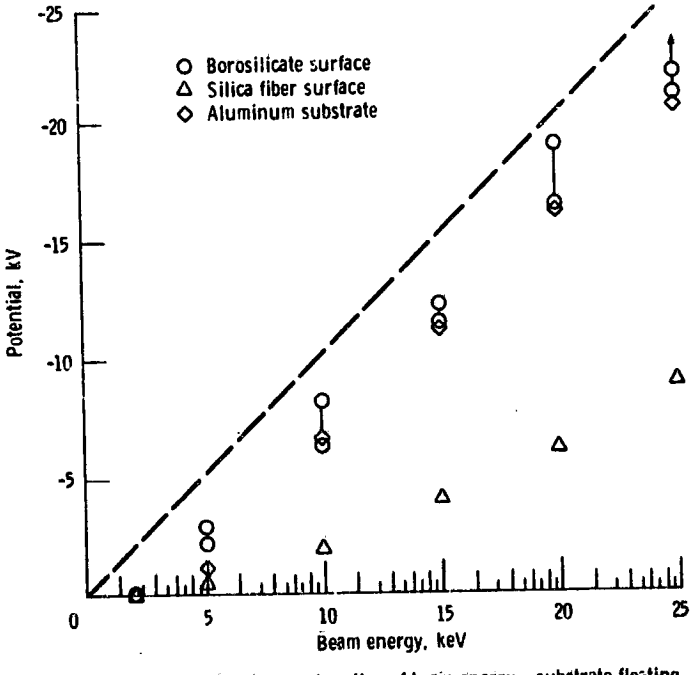

Figure 17. - Potential as a function of beam energy - substrate floating.

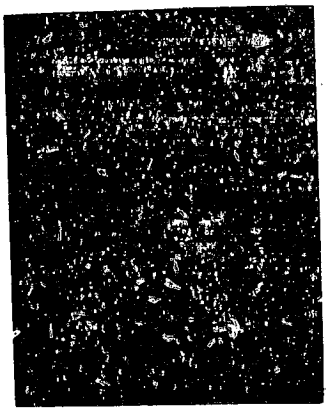

Figure 18. - 15-Minute time exposure of edge-irradiated specimen - substrate floating. Beam energy, 25 keV; flux, 1 nA/cm^2.